1   **The additionality problem of Ocean Alkalinity Enhancement**

3   Lennart Thomas Bach

5   Institute for Marine and Antarctic Studies, University of Tasmania, Hobart, TAS, Australia.

7   *Correspondence to*: Lennart Bach (Lennart.bach@utas.edu.au)

10   **Abstract.** Ocean Alkalinity Enhancement (OAE) is an emerging approach for atmospheric carbon

11   dioxide removal (CDR). The net climatic benefit of OAE depends on how much it can increase CO_2

12   sequestration relative to a baseline state without OAE. This so-called 'additionality' can be calculated

13   as:

15   Additionality $= C_{OAE} - \Delta C_{baseline}$

17   So far, feasibility studies on OAE have mainly focussed on enhancing alkalinity in the oceans to

18   stimulate CO_2 sequestration (C_{OAE}) but not primarily how such anthropogenic alkalinity would modify

19   the natural alkalinity cycle and associated baseline CO_2 sequestration ($\Delta C_{baseline}$). Here, I present

20   incubation experiments where materials considered for OAE (sodium hydroxide, steel slag, olivine) are

21   exposed to beach sand to investigate the influence of anthropogenic alkalinity on natural alkalinity

22   sources and sinks. The experiments show that anthropogenic alkalinity can strongly reduce the

23   generation of natural alkalinity, thereby reducing additionality. This is because the anthropogenic

24   alkalinity increases the calcium carbonate saturation state, which reduces the dissolution of calcium

25   carbonate from sand, a natural alkalinity source. I argue that this 'additionality problem' of OAE is

26   potentially widespread and applies to many marine systems where OAE implementation is considered

27   – far beyond the beach scenario investigated in this study. However, the problem can potentially be

28   mitigated by dilute dosing of anthropogenic alkalinity into the ocean environment and avoid OAE at

29   hotspots of natural alkalinity cycling such as in marine sediments. Understanding a potential slowdown

30   of the natural alkalinity cycle through the introduction of an anthropogenic alkalinity cycle will be

31   crucial for the assessment of OAE.

33   1. **Introduction**

34

35   Keeping global warming between 1.5 to 2°C requires rapid reduction of greenhouse gas emissions and

36   gigatonne-scale atmospheric carbon dioxide removal (CDR), using a portfolio of terrestrial and marine

37   CDR methods (Nemet et al., 2018). Ocean alkalinity enhancement (OAE) is considered as an important

CDR method of the marine portfolio (Hartmann et al., 2013). OAE can be achieved through a variety of geochemical and electrochemical processes (Renforth and Henderson, 2017). All of them enhance surface ocean alkalinity to reduce the hydrogen ion (H^+) concentration in seawater (i.e., increase pH). This reduction in $[H^+]$ causes a shift in the carbonate chemistry equilibrium:

$$CO_2 + H_2O \leftrightarrow H^+ + HCO_3^- \leftrightarrow 2H^+ + CO_3^{2-} \tag{1}$$

from CO_2 on the left towards bicarbonate (HCO_3^-) and carbonate ion (CO_3^{2-}) on the right. The associated reduction of the CO_2 partial pressure in seawater (pCO_2) enables atmospheric CO_2 influx into the oceans (or reduces CO_2 outflux if $pCO_2 >$ atmospheric pCO_2). This transfer (retention) of atmospheric CO_2 into the ocean leads to an increase of the dissolved inorganic carbon (DIC) concentration in seawater, with DIC defined as:

$$DIC = [CO_2] + [HCO_3^-] + [CO_3^{2-}] \tag{2}$$

Among the widely discussed OAE approaches are coastal enhanced weathering and electrodialytical acid removal (Eisaman et al., 2023). Coastal enhanced weathering achieves alkalinity increase via the addition of pulverized alkaline rocks like limestone, olivine, or alkaline industrial products like steel slag to coastal environments (Meysman and Montserrat, 2017; Feng et al., 2017; Harvey, 2008; Schuiling and Krijgsman, 2006; Renforth, 2019).

Electrodialytical OAE is somewhat different from coastal enhanced weathering since no materials are added to seawater. Instead, water dissociation into H+ and OH- is catalyzed in bipolar membranes, and these ions are then separated using electrical energy and ion-selective membranes (de Lannoy et al., 2018). H^+ is captured as hydrochloric acid whilst OH- is captured as sodium hydroxide (NaOH). The hydrochloric acid needs to be utilised, neutralized in deep ocean sediments, or stored in save reservoirs outside the ocean (Eisaman et al., 2018; Tyka et al., 2022). NaOH is enriched in the processed seawater, which is released back into the surface to convert CO_2 into HCO_3^- (Eisaman et al., 2018; Tyka et al., 2022).

A critical side-effect of OAE is the associated increase in CO_3^{2-} concentrations, which comes through the shift in the marine carbonate equilibrium through H^+ absorption (see above). This increase elevates the saturation state for calcium carbonate (Ω_{CaCO3}), the metric which determines the solubility of $CaCO_3$ in seawater. Ω_{CaCO3} is defined as:

$$\Omega_{CaCO3} = \frac{[Ca^{2+}]_{SW} \times [CO_3^{2-}]_{SW}}{K_{sp}} \tag{3}$$

73 where $[Ca^{2+}]_{sw}$ and $[CO_3^{2-}]_{sw}$ are calcium ion (Ca^{2+}) and CO_3^{2-} concentration in seawater and K_{sp} is the

74 empirically determined solubility product (Mucci, 1983). K_{sp} differs for different crystal forms of

75 $CaCO_3$. It is higher for Aragonite than for Calcite, meaning Aragonite is more soluble (Mucci, 1983).

76 Aragonite (Arg) and Calcite (Cal) precipitation is thermodynamically favoured when Ω_{Arg} and Ω_{Cal} are

77 ≥ 1 (Adkins et al., 2020). $CaCO_3$ precipitation is of high relevance for the assessment of OAE as the

78 drawdown of CO_3^{2-} through precipitation reduces alkalinity, shifts the carbonate chemistry equilibrium

79 (eq. 1) towards CO_2 and thus counters the CDR efficiency of OAE (Moras et al., 2022; Fuhr et al., 2022;

80 Hartmann et al., 2023).

81 Logistical constraints suggest that OAE would at least initially more likely to be conducted in

82 coastal environments (Renforth and Henderson, 2017; Lezaun, 2021; He and Tyka, 2023). Here,

83 alkalinity-enhanced seawater would likely be in contact with marine sediments (Meysman and

84 Montserrat, 2017; Feng et al., 2017; Harvey, 2008). The highly abundant particles in marine sediments

85 can serve as nuclei for $CaCO_3$ precipitation thereby catalysing alkalinity loss when Ω_{CaCO3} is ≥ 1 (Zhong

86 and Mucci, 1989; Morse et al., 2003; Adkins et al., 2020). This constitutes a problem for OAE because

87 alkalinity-enhanced seawater with its high Ω_{CaCO3} is then exposed to particles that catalyse precipitation.

88 Indeed, recent studies have demonstrated that this particle-catalysed precipitation can rapidly reduce

89 alkalinity, with the degree and rate of alkalinity reduction depending on the amount of alkalinity added

90 and the particle concentrations (Moras et al., 2022; Fuhr et al., 2022; Hartmann et al., 2023).

91 Particle-catalysed $CaCO_3$ precipitation has received significant consideration as a loss term for OAE

92 efficiency (Renforth and Henderson, 2017; Moras et al., 2022; Fuhr et al., 2022; Hartmann et al., 2013,

93 2023). However, there is another complication affecting OAE efficiency near sediments, which has

94 received no attention and will be in focus of this study. Sediments can not only provide precipitation

95 nuclei but also constitute natural alkalinity sources, for example via dissolution of $CaCO_3$ or other

96 carbonates (Torres et al., 2020; Wallmann et al., 2022; Krumins et al., 2013; Aller, 1982; Middelburg

97 et al., 2020). Sandy beaches can be rich in biogenic carbonates and organic matter thereby creating

98 environments of high respiratory CO_2. Accordingly, Ω_{CaCO3} is low close to the sediments or within pore

99 waters and $CaCO_3$ dissolution is favoured (Liu et al., 2021; Perkins et al., 2022; Reckhardt et al., 2015).

100 This form of natural alkalinity formation via $CaCO_3$ dissolution can sequester CO_2 which may have

101 otherwise be released into the atmosphere (Saderne et al., 2021; Krumins et al., 2013; Aller, 1982;

102 Fakhraee et al., 2023; Archer et al., 1998). OAE within these naturally low Ω_{CaCO3} environments could

103 have two effects. First, it would have the desired effect of consuming H^+ and increasing CO_2

104 sequestration via the generation of anthropogenic alkalinity. Second, the consumption of H^+ would

105 increase Ω_{CaCO3}, which could reduce the dissolution of $CaCO_3$ and thus reduce natural CO_2 sequestration

106 since less natural alkalinity is produced. Due to this second effect, the first (desired) effect of CO_2

107 sequestration may be significantly reduced. Accordingly, the net gain in CO_2 sequestration would be

108 lower than one would have hoped for.

109   The concept "additionality" describes the net gain in CO_2 sequestration achieved through the
110 implementation of a CDR method relative to a hypothetical baseline (or "business-as-usual") scenario
111 (Michaelowa et al., 2019). Per definition, "additional" is all CO_2 sequestration achieved through the
112 implementation of a CDR method (here OAE) that goes beyond natural and anthropogenic CO_2
113 sequestration that already occurs in the baseline scenario without the implementation of the CDR
114 method. Additionality is a central concept in climate policy that has been utilized for carbon accounting
115 in the Clean Development Mechanism established under the 1997 Kyoto Protocol (Havukainen et al.,
116 2022). It can be defined in simple terms as:

117

118   Additionality $= C_{OAE} - \Delta C_{baseline}$ (4)

119

120 where C_{OAE} is the CO_2 sequestration achieved through OAE, and $\Delta C_{baseline}$ is the change in the baseline
121 CO_2 sequestration through the implementation of OAE.

122   This study aims to reveal and describe how anthropogenic alkalinity affects natural alkalinity
123 release to better understand the CO_2 sequestration potential of OAE in the context of additionality. I
124 present observational data and three experiments where three types of anthropogenic alkalinity sources
125 (NaOH, steel slag, olivine) are exposed to a natural alkalinity source and sink (beach sand) to investigate
126 their interactions. Afterwards, I examine these interactions (termed "additionality problem"), discuss
127 their relevance, and how it could be managed.

128

129   **2. Methods**

130

131   **2.1. Carbonate chemistry and dissolved silicate transects along Southern Tasmanian**
132   **beaches**

133

134 The project was initialised with near-shore alkalinity, pH, and dissolved silicate ($Si(OH)_4$) transects on
135 four Tasmanian beaches to determine whether these beaches are detectable alkalinity sinks or sources.
136 The investigated beaches were Clifton South, Clifton North, Goats, and Wedge on the Southarm near
137 Hobart (Tasmania; Fig. 1, Table S1).

138   Samples for alkalinity and $Si(OH)_4$ were taken by filling 200 mL seawater from 0.2 m depth
139 into a polyethylene (PE) bottle. Samples for pH were collected in a 60 mL polystyrene (PS) jars filled
140 and closed at 0.2 m depth. Both the PE bottles and the PS jars were pre-rinsed with sample. The sample
141 closest to shore was taken in the swash zone (zone where wave bores run up and down the beach) at the
142 spot where a wave bore reached highest within ~5 minutes of observation. A ~0.2 m deep hole was dug
143 (Fig. 1) and water was collected from the groundwater with a 60 mL syringe. The second sample was
144 from the upper part of the swash zone where waves pushed water up the beach. Samples further out
145 were taken from within the wave breaking zone to about 50-100 m beyond the wave breaking zone.

146 Samples were taken by walking into the water to the point it became too deep and a surfboard was used
147 as sampling vehicle.

148 The samples were transported back to the beach where pH was measured within 15 minutes
149 after sampling as described in section 2.4. Alkalinity and Si(OH)$_4$ samples were filtered after pH
150 measurements with a 0.22 syringe filter (nylon membrane) into a 125 mL PE bottle (alkalinity) or 60
151 mL PS plastic jar (Si(OH)$_4$). Both containers, the syringe, and the syringe filter were pre-rinsed with
152 sample.
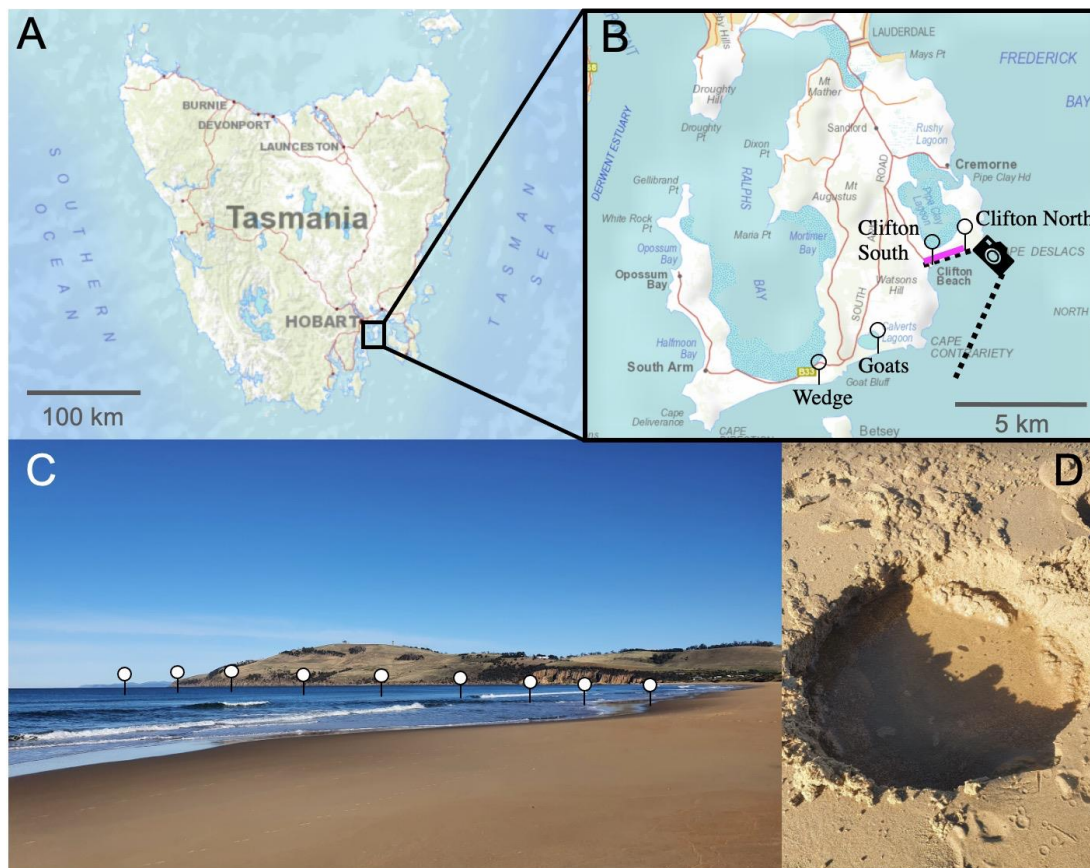
153

154 **Figure 1**. Locations of the beach transects and beach sand sampling in Tasmania. (A) Map of Tasmania
155 with (B) enlarged map of the Southarm region south of Hobart. Needles show locations the beach
156 transects and the pink line along Clifton Beach shows where sand samples (Sand 1-5) were collected
157 for incubation experiments. The camera symbol illustrates the position from where the picture shown
158 in panel (C) was taken. (C) illustrates approximate location of one of the beach transects. (D) A hole
159 that was dug to sample seawater just above the swash zone, i.e., the first sample location along the
160 transects from the beach towards 150-200 m offshore. The maps were reproduced with the permission
161 of the Environment Heritage and Land Division, Department of Natural Resources and Environment
162 Tasmania, © State of Tasmania.

163

164 **2.2. Laboratory experiments**

165

2.2.1. Experiment 1: Replicated dissolution assays to monitor interaction between beach sand and alkaline materials

Experiment 1 was designed to investigate the interaction between 4 different beach sands and alkaline materials during the incubation in seawater. The experiment required 60 HDPE bottles, each with a volume of 125 mL. These 60 bottles were thoroughly cleaned with double-deionised water and dried at 60°C. Twelve bottles were filled with sand from one of the 4 sampling locations (section 2.3.), respectively (totalling 48 bottles). Another set of 12 bottles were not filled with sand. This yielded 5 sets of 12 bottles (Fig. 2). Of each set, 3 bottles remained without further addition, 3 received 51.3 µL of 1 molar NaOH (targeted alkalinity increase was 428 µmol/kg), 3 received 0.0065 g of ground steel slag, and 3 received 1 g of ground olivine (Fig. 2; sand, steel slag, and olivine properties were determined as described in section 2.3.). The 48 bottles that contained sand were filled with 10 g of sand if slag or NaOH was added or 9 g of sand if olivine was added. This was done so that the weights of added sand plus alkalinity feedstock was always ~10 g.

Once the solid components were added, each bottle was filled with 120 (+/-4) g of seawater (Salinity =35 ±0.2, alkalinity = 2259.7 µmol/kg) collected in July 2022 in the Derwent Estuary near Taroona. Salinity and pH of the seawater was determined a few minutes before transfer into the incubation bottles with a Metrohm 914 pH/conductivity meter as described in section 2.4. The transfer of the seawater into the incubation bottles took 30 minutes in total (please note that in the case of NaOH additions, seawater was added to the bottles before 51.3 µL of 1 molar NaOH was added). The incubation bottles were immediately mounted on a plankton wheel (1.06 m diameter, 2 rounds per minute), which was placed in a temperature-controlled room set to 15°C (Fig. S1). The plankton wheel kept the various mixtures of sand, alkalinity source, and seawater moving inside the bottles. The experiment commenced at 16:00 on the 17th of August, 2022.

After ~6.8 days (24th of August), bottles were consecutively removed from the plankton wheel in random order between 8:00 and 15:30. pH was measured inside the bottle with a pH electrode, directly after a bottle was taken off the plankton wheel. Afterwards, the alkalinity sample was filtered with a syringe through a 0.2 µm nylon filter into a dry and clean 125 mL HDPE bottle and stored in the dark at 7°C.

2.2.2. Experiment 2: Alkalinity formation at Omega gradients

Experiment 2 was designed to investigate whether a decline of Ω_{CaCO_3} enhances the formation of natural alkalinity via $CaCO_3$ dissolution and how anthropogenic alkalinity sources (olivine, slag, NaOH) influence this process. The experiment required 60 HDPE bottles (125 mL) cleaned with acid and double-deionised water (note that acid was used in Experiment 2 to make sure all remnants from Experiment 1 were washed out of the bottles). All 60 incubation bottles were filled with sand from

203   Clifton Beach (section 2.3.). The treatments were then set up as follows: Twelve bottles were filled only

204   with 10 g of sand; Twelve with 10 g of sand and 0.006515 (+/-0.00007) g steel slag; Twelve with 9 g

205   of sand and 1 (+/-0.002) g of olivine; Eight with 10 g of sand at "un-equilibrated" NaOH addition;

206   Sixteen with 10 g of sand at "equilibrated" NaOH addition (Fig. 2).

207   For each treatment, a gradient in seawater CO_2 concentrations was established from bottle 1 (lowest

208   CO_2) to bottle 8-16 (highest CO_2). This was achieved with the following approach: A batch of seawater

209   (Salinity= 35±0.2, alkalinity = 2266.8 µmol/kg) was collected in November 2022 in the Derwent

210   Estuary near Taroona. About 0.3L of the batch was bubbled with pure CO_2 gas for about 5 minutes to

211   generate highly CO_2-enriched seawater. Another ~7L of the batch was used as source water to fill the

212   incubation bottles. pH and temperature were measured in this batch prior to filling the incubation

213   bottles. The low CO_2 incubation bottles (bottle 1 in the sequence from e.g. 1 to 12, Fig. 2) were then

214   filled first. Afterwards, about 20 mL of the CO_2-enriched seawater was added to the ~7L batch. The

215   batch was shaken thoroughly to mix the seawater with the CO_2-enriched seawater and the pH and

216   temperature were measured again. Once a stable pH/temperature reading was achieved, (bottle 2) was

217   filled. This procedure was repeated until all bottles in a treatment were filled and a CO_2 (and DIC)

218   gradient was established across the incubation bottles. For the equilibrated and un-equilibrated NaOH

219   treatments, I followed the same procedure but separate 0.3L and 7L batches were used for the CO_2

220   enrichment that had previously been amended with NaOH to elevate alkalinity from 2266.8 to 2757.4

221   µmol/kg prior to filling the incubation bottles. All 60 bottles were filled with 120 +/-4 g of seawater

222   and immediately mounted on the plankton wheel (2nd of December, 2022; 17:00) under the same

223   conditions as in Experiment 1 (i.e. 15°C, 2 rounds per minute, Fig. S1).

224   After ~6.8 days (9th of December), bottles were removed from the plankton wheel between 9:00 and

225   16:00. pH and alkalinity were sampled as described in section 2.2.1.

226

227   **2.2.3.   Experiment 3: pH dependency of alkalinity formation from slag and olivine**

228

229   Experiment 3 was designed to investigate whether a lower seawater pH would promote alkalinity

230   formation from steel slag and olivine.

231   The experiment required 12 new HDPE bottles (125 mL) cleaned with double-deionised water and

232   dried thereafter. Six of the 12 bottles were filled with 0.00644 (±0.00007) g steel slag and the other six

233   with 1.0003 (±0.002) g of olivine. Three slag and three olivine bottles were filled with seawater from

234   the same seawater source as used in Experiment 2 (Salinity=35±0.2, alkalinity=2263.2 µmol/kg, pH

235   (total scale) = 7.82). pH and temperature were measured prior to filling the bottles with seawater

236   (section 2.4.). Afterwards, the ~2L seawater batch was amended with about 80 mL of CO_2-enriched

237   seawater as explained in section 2.2.2. This enrichment lowered the pH_T (total scale) from 7.82 to 6.85.

238   This low pH_T (high CO_2) seawater was used to fill the other 3 slag and olivine incubation bottles. The

239   12 bottles with 122.8 (±0.15) g of seawater were immediately mounted on the plankton wheel (Fig. S1)

240   after filling (16th of December, 2022; 16:40) under the same conditions as in Experiment 1 and 2 (i.e.

241   15°C, 2 rounds per minute).

242   After ~6.8 days (23rd of December), the 12 bottles were randomly removed from the plankton wheel

243   between 9:00 and 11:00. pH and alkalinity were sampled as described in section 2.2.1.

244
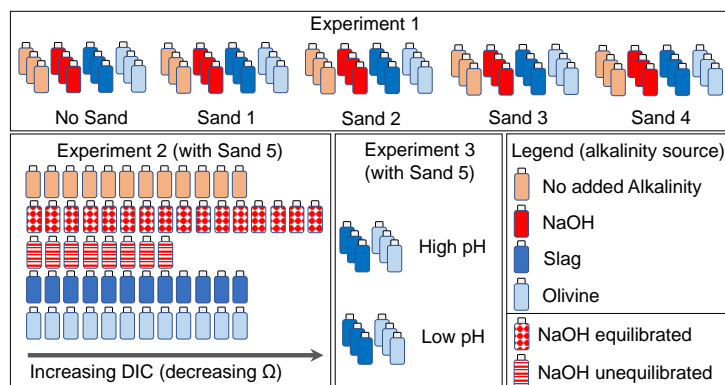
246   **Figure 2**. Design of Experiments 1, 2, and 3. Bottles represent treatments with incubation of seawater,

247   sand, and alkalinity sources (colour code represents alkalinity source). In Experiment 2, NaOH was

248   used as alkalinity source in two explicit scenarios as described in section 2.2.2.

249

250   **2.3. Preparation and characterization of alkaline materials and beach sand**

251

252   In total, 5 sand samples (0.5-1kg) were collected for Experiments 1 and 2 at Clifton Beach, Tasmania

253   (Fig. 1, Table S2). Sampling permission was granted by the Department of Natural Resources and

254   Environment (Authority No. ES 22314). Wet sand was sampled on the upper end of the swash zone and

255   stored in zip bags at 15°C. Samples 1-4 were used for Experiment 1, ~24 hours after sampling while

256   sample 5 was used for Experiment 2, ~72 hours after sampling.

257   Olivine rocks were sourced from the Mount Shadwell Quarry in Mortlake (Australia, Table S2). Basic

258   oxygen slag (hereafter just called slag) was sourced from the Liberty Primary Steel – Whyalla

259   Steelworks (Australia, Table S2). Olivine rocks and slag (Fig. S2) were crushed with a hydraulic crusher

260   into smaller pieces of about 10 mm and then milled with a ring mill in a chrome milling pot to yield

261   particle size distributions as shown in Fig. S3.

262   Wet and dry weight of the sand used for laboratory experiments was determined by weight difference

263   of a wet and a dry sample. The wet sample (~80 g) was put into a clean plastic jar and dried for 24-72

264   hours at 60°C. The particle size spectra of the 5 dried sand samples as well as slag and olivine mineral

265   were determined with a Sympatec QICPIC particle imager.

266   For total particulate carbon (TPC) and particulate organic carbon (POC) analyses, dried sand samples

267   were milled for 12 minutes in a Retsch MM200 ball mill. Between 4-10 mg of each of the pulverized

268   sand samples were weighed into 10 tin cups for TPC or 10 silver cups for POC (2 TPC and POC

269   replicates for each sample). The POC samples were moisturized with 50µL of MilliQ water, placed for

18 hours in a dessicator that contained 36% HCl to remove all carbonates and then dried. TPC and POC samples were analysed for carbon content using a Thermo Finnigan EA 1112 Series Flash Elemental Analyser. Particulate inorganic carbon (PIC) content of the samples was then calculated as the difference between TPC and POC. Percent content of carbonates was estimated by multiplying % PIC content by the molecular weight of $CaCO_3$ (100 g/mol) and $MgCO_3$ (84.3 g/mol) for upper and lower estimates.

2.4. Carbonate chemistry, salinity, and $Si(OH)_4$ measurements

pH was determined potentiometrically using a Metrohm 914 pH meter following Standard Operation Procedure 6a described in Dickson et al., (2007) but omitting the test for ideal Nernst behaviour of the electrode (ideal Nernst behaviour was assumed). A new pH electrode (Metrohm Aquatrode Plus) was calibrated on the total pH scale (pH_T) with certified reference material (CRM) TRIS buffer (batch #37), provided by Prof. Andrew Dickson's laboratory. The calibration procedure for the relevant temperature range (~8 – 18°C) followed the exact workflow as described by Ferderer et al., (2022). Precision of the pH measurement was assumed to be ±0.015 based on experience with the probe.

Alkalinity was determined in an open cell titration following Dickson et al., (2003). Samples were measured in duplicate (each ~60 g) with a Metrohm 811 titration unit equipped with a Metrohm Aquatrode Plus. Alkalinity was calculated from titration curves using the Calkulate function of PyCO2sys (Humphreys et al., 2020). The difference in alkalinity between duplicate titrations of the sample was on average 1.95 µmol/kg and >75% were within 4 µmol/kg (N=185), which was assumed to be the precision of the measurement (±2 µmol/kg). Accuracy was controlled by correcting alkalinity values with CRM provided by A.G. Dickson's laboratory. Alkalinity was measured within maximally 20 days after sampling.

Salinity was measured with a Metrohm conductivity probe with a PT1000 temperature sensor connected to a Metrohm 914 conductivity meter. The probe was calibrated with DIC/alkalinity CRM from A.G. Dickson's laboratory for which a salinity of 33.464 has been reported (CRM batch 200). Conductivity was measured in mS/cm^2 and salinity was subsequently calculated on the practical salinity scale following Lewis and Perkin, (1978), following the workflow described by Moras et al., (2022). A relatively low precision of +/- 0.2 was determined from repeat measurements, although precision was likely lower under field conditions where there was no temperature control.

Si concentrations for beach transects were measured 18 hours after sampling following Hansen and Koroleff, (1999). No Si measurements were conducted for Experiments 1-3.

2.5. Carbonate chemistry calculations

306 Carbonate chemistry conditions were calculated with the "carb function" in Seacarb (Gattuso et al.,
307 2021), with pH_T, alkalinity, salinity, temperature, phosphate and $Si(OH)_4$ concentrations as input
308 variables, stoichiometric equilibrium constants from (Lueker et al., 2000), and default settings for the
309 other equilibrium constants. Si was not measured due to volume limitations, so I assumed a value of 50
310 μmol/kg at the end of the experiments, when either sand, olivine, or slag were incubated. Likewise,
311 phosphate was not measured and I assumed 2 μmol/kg at the end of the experiments when slag was
312 incubated. These Si and phosphate releases were based upon previous trials. Note, however, that
313 concentrations of Si and phosphate within these ranges have negligible impact on calculated carbonate
314 chemistry parameters (e.g., pCO_2 changes by ~1 μatm when Si is assumed to be 0 instead of 50
315 μmol/kg).

316 Propagated errors in derived carbonate chemistry parameters (e.g., DIC) were calculated with
317 the "errors" function in Seacarb using measurement precisions described in section 2.4. for pH_T
318 (±0.015), alkalinity (±2 μmol/kg), and salinity (±0.2), default uncertainties for equilibrium constants
319 and temperature, and when applicable (see above) ±50 μmol/kg for $Si(OH)_4$ and ±2 μmol/kg for
320 phosphate.

321

322 **2.6. Calculations of the CO_2 uptake ratio (η_{CO2}) for carbonate and non-carbonate**
323 **alkalinity sources**

324

325 The atmospheric CO_2 uptake ratio for OAE (η_{CO2}) was defined as the number of moles DIC (ΔDIC)
326 absorbed per number of moles alkalinity added (ΔAlkalinity) (Tyka et al., 2022).

327

328 $$\eta_{CO2} = \frac{\Delta DIC}{\Delta Alkalinity} \hspace{4cm} (5)$$

329

330 η_{CO2} was shown to range roughly between 0.75 and 0.9 mol:mol in the surface ocean (Schulz et al.,
331 2023; Tyka et al., 2022). However, this η_{CO2} range only applies for alkalinity source materials that
332 exclusively increase alkalinity without a concomitant increase in DIC when they are added to seawater
333 ($Alk_{non-carbonate}$). Such sources comprise for example NaOH, slag, and olivine. The estimated range does
334 not apply when all or fractions of the added alkalinity comes from carbonates ($Alk_{carbonate}$), since $CaCO_3$
335 contributes 2 moles of alkalinity and 1 mole of (non-atmospheric) DIC when they dissolve. In the
336 following three paragraphs I describe how η_{CO2} was calculated when considering varying contributions
337 of $Alk_{non-carbonate}$ and $Alk_{carbonate}$ for a hypothetical or observed increase of ΔAlkalinity. Please note that
338 the sum of $Alk_{carbonate}$ and $Alk_{non-carbonate}$ always equals ΔAlkalinity. Please also note that η_{CO2} was
339 calculated in different ways for a hypothetical case and Experiment 1 (i.e. η_{CO2} still has the same
340 theoretical meaning as defined in eq. 5 but was estimated in different ways).

341 The dependency of η_{CO2} on the relative contribution of $Alk_{carbonate}$ and $Alk_{non-carbonate}$ was calculated as:

342

343 $$\eta_{CO2} = \frac{DIC_{equilibrated} - \left(\frac{Alk_{carbonate}}{2}\right) - DIC_{initial}}{Alk_{non-carbonate} + Alk_{carbonate} - Alk_{initial}} \qquad (6)$$

344

345 where $DIC_{initial}$ and $Alk_{initial}$ are DIC and alkalinity in seawater before alkalinity was increased, assuming

346 a seawater pCO_2 in equilibration with the atmosphere. $DIC_{equilibrated}$ is the amount of DIC from the

347 environment (e.g. from the atmosphere) that can be stored in seawater after the increase of $Alk_{carbonate}$

348 and $Alk_{non-carbonate}$, assuming seawater pCO_2 in equilibrium with the atmosphere. η_{CO2} was first

349 calculated for a theoretical case where $Alk_{initial}$ was 2350 µmol/kg and $DIC_{initial}$ was calculated for the

350 surface ocean (15°C, Salinity = 35, carbonate chemistry constants as in section 2.5), assuming a pCO_2

351 of 420 µatm. $Alk_{carbonate}$ and $Alk_{non-carbonate}$ were then varied in a range of scenarios (from 0 to 100%

352 $Alk_{carbonate}$) to increase the sum of them by 1 µmol/kg. η_{CO2} was calculated for each scenario.

353 Next, η_{CO2} was calculated specifically for Experiment 1 as follows: ΔAlkalinity was higher in the NaOH

354 and slag treatments when no sand was present compared to incubations with sand (section 3.2).

355 ΔAlkalinity was very likely $Alk_{non-carbonate}$ in all incubations while the reduced ΔAlkalinity in the

356 incubations with sand was likely due to secondary precipitation of carbonates (section 4.2.1). Based on

357 these conclusions, η_{CO2} was estimated for Experiment 1 as:

358

359 $$\eta_{CO2} = \frac{(\Delta Alkalinity_{no-sand} - \Delta Alkalinity_{sand}) \times 0.5 + \Delta Alkalinity_{sand} \times 0.86}{\Delta Alkalinity_{no-sand}} \qquad (7)$$

360

361 where $\Delta Alkalinity_{no-sand}$ and $\Delta Alkalinity_{sand}$ are the changes in alkalinity measured in incubations

362 without sand and with sand, respectively; 0.5 is the η_{CO2} when $Alk_{non-carbonate}$ is lost via the precipitation

363 of carbonates where 2 moles of alkalinity and 1 mol of DIC are sequestered; 0.86 is the η_{CO2} when all

364 ΔAlkalinity is $Alk_{non-carbonate}$ under the conditions set up in the experiments (i.e. 15°C, salinity=35; see

365 above). Please note that ΔAlkalinity was higher in the olivine incubations when sand was present, which

366 is opposite to the NaOH and slag incubations for reasons discussed in section 4.2.1. Therefore, η_{CO2}

367 was calculated assuming all ΔAlkalinity was $Alk_{non-carbonate}$ for the olivine incubations (i.e. $\eta_{CO2} = 0.86$).

368 For the incubations without an added alkalinity source all ΔAlkalinity was assumed to be $Alk_{carbonate}$ so

369 that η_{CO2} was 0.36. This assumption is justified with a 2:1 mol:mol ΔAlkalinity:ΔDIC release ratio as

370 observed in Experiment 2 (see next paragraph).

371 η_{CO2} was also specifically calculated for Experiment 2. This required knowledge of how much of the

372 measured ΔAlkalinity was contributed by $Alk_{carbonate}$ and $Alk_{non-carbonate}$. In the treatments where only

373 sand was incubated, alkalinity and DIC increased roughly in a 2:1 molar ratio over the course of the

374 experiment (i.e. ΔAlkalinity:ΔDIC = 2:1 mol:mol). Thus, it can be assumed that most of the measured

375 alkalinity increase is $Alk_{carbonate}$. In contrast, when sand was incubated with alkaline materials, alkalinity

376 and DIC generally increased with a molar ratio that was >2:1 because alkaline materials release

377 alkalinity without a concomitant increase of DIC. Based on these constraints, we can roughly

378 approximate the contribution of $Alk_{carbonate}$ and $Alk_{non-carbonate}$ to the measured alkalinity increase

379 (ΔAlkalinity) as:

380

381 $$\%Alk_{carbonate} = 1/\left(\left(\frac{\Delta Alkalinity}{\Delta DIC}\right)/2\right) \times 100 \qquad (8)$$

382

383 Where $\%Alk_{carbonate}$ is the percentage contribution of $Alk_{carbonate}$ to ΔAlkalinity. Based on eq. (8), a

384 ΔAlkalinity:ΔDIC of for example 8:1 mol:mol would suggest that 25% of the ΔAlkalinity is $Alk_{carbonate}$

385 and the other 75% $Alk_{non-carbonate}$. $Alk_{carbonate}$ and $Alk_{non-carbonate}$ were calculated with eq. 8 for all

386 incubations in Experiment 2 and this information was then used to calculate η_{CO2} with eq. (6). Finally,

387 the amount of DIC that can be stored in seawater due to an increase of $Alk_{carbonate}$ and $Alk_{non-carbonate}$

388 (DIC_{OAE}) was calculated as:

389

390 $$DIC_{OAE} = \eta_{CO2} * \Delta\text{Alkalinity} \qquad (9)$$

391

392 for experiment 2.

393

394 **2.7. Statistical analysis**

395

396 Experiment 1 and 3 were analysed with a two-way analysis of variance (ANOVA) where either "sand"

397 and "alkalinity source material" (Experiment 1) or "carbonate chemistry" and "alkalinity source

398 material" (Experiment 3) were defined as independent variables. The dependent variables were the

399 changes in carbonate chemistry (e.g. ΔAlkalinity) over the course of the incubations. Homogeneity of

400 variance was assessed by visually inspecting if plotted model residuals vs. fitted values were scattering

401 similarly around 0. Normality of the residuals was assessed by inspecting qqplots where theoretical

402 quantiles plotted against standardized residuals should ideally resemble a straight line. Such a straight-

403 line appearance (i.e. ideal normality) was not always given, so some datasets were rank-transformed.

404 However, transformation did not improve normality substantially so that non-transformed data was

405 used for all analyses. Statistical differences between individual treatments were assessed with a Tukey

406 post-hoc test. Significant differences were assumed when $p < 0.05$.

407 Experiment 2 was analysed by plotting ΔAlkalinity for each alkalinity source material and sand against

408 the increase in DIC that was established via additions of CO_2-saturated seawater (section 2.2.2). The

409 data was fitted with the polynomial equation $ax^2 + bx + c$, where x is the amount of DIC added to each

410 treatment and a, b, c are fit parameters. To estimate additionality of ΔAlkalinity and DIC_{OAE}, the curve

411 fitted to the sand-only data was compared to the curves fitted to the treatments.

412

3. Results

3.1. Beach transects

Beach transects consisted of 8-9 sampling points from just above the swash zone to 150-220 m offshore at four locations (Table S1, Fig. 1). Alkalinity showed distinct patterns across the locations. At Clifton South and Wedge, alkalinity was higher in the swash zone than in the open water. This was particularly pronounced at Clifton South with a value of 2418 µmol/kg relative to open water values of about 2300 µmol/kg (Fig. 3A). At Goats Beach, no such alkalinity gradient was observed across the transect, while alkalinity was lower in the swash zone at Clifton North (Fig. 3A). Wedge differed to the other locations in that alkalinity was generally lower (~2160 compared to ~2300 µmol/kg in open water).

pH_T was lowest in samples just above the swash zone at all four locations (Fig. 3B). The difference relative to open water was most pronounced at Clifton South with pH_T of 7.76 just above the swash zone compared to approximately 8.05 in the open water, while least pronounced at Goats. Gradients at Clifton North and Wedge were in between these two extremes. pH_T at Wedge was on average higher in the open water than at the other locations, i.e. 8.08 compared to 8.05 (Fig. 3B).

$Si(OH)_4$ concentrations were highest in samples from just above the swash zone at all four locations (Fig. 3C). The most pronounced gradient was observed at Clifton South, with $Si(OH)_4$ of 8.6 µmol/L just above the swash zone and ~1.6 µmol/L in open water. The least pronounced gradient was observed at Goats, and intermediate gradients at Clifton North and Wedge (Fig. 3C).

Overall, the data shows consistency across the three parameters measured in that Clifton South showed most pronounced trends, Goats the least pronounced trends, and Clifton North and Wedge being in between (Fig. 3).

436
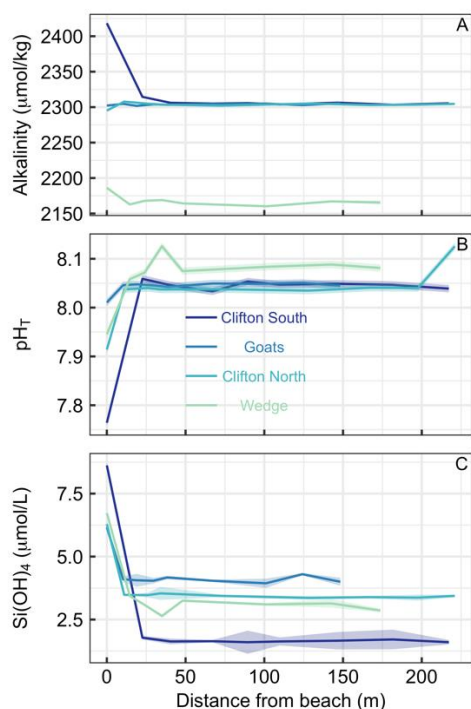
Figure 3. Transects of (A) alkalinity, (B) pH_T, and (C) $SiOH_4$ at four different beach locations in southern Tasmania (see Table S1 and Fig. 1 for locations). The first sampling was at the upper end of the swash zone and then 7-8 more samples were taken until 150-200 m offshore. Lines and shaded areas show averages and uncertainties, respectively.

3.2. Experiment 1

Alkalinity increased over the course of the 6.8 days in all treatments where alkaline materials were added (Fig. 4). Changes in alkalinity (ΔAlkalinity) were between ~610-400 µmol/kg for the slag, ~420-290 µmol/kg for the NaOH, and 280-370 µmol/kg for the olivine treatment. In contrast, ΔAlkalinity changed very little (i.e., ΔAkalinity $\leq$6 µmol/kg) when no alkaline materials were added. (Please note that an important outlier was observed in Sand 2 where ΔAlkalinity was 87.3 µmol/kg which will be discussed in section 4.2.2.). The two-way ANOVA revealed significant effects of (1) the type of sand, (2) the type of alkalinity source, and (3) the interaction of these two on ΔAlkalinity ($p<0.05$). For the slag and the NaOH treatment, ΔAlkalinity was significantly higher when these were incubated without sand but only small differences were observed across the four sand samples. In contrast, ΔAlkalinity was slightly lower in the olivine treatment when no sand was present during incubations although the difference was only significant relative to olivine incubated in Sand 4 (Fig. 4A).

Changes in pH_T (ΔpH_T) reflected the patterns described for ΔAlkalinity (Fig. 4B). ΔpH_T was highest in the slag and the NaOH treatment when no sand was added, while this difference between the presence and absence of sand was not observed for olivine. ΔpH_T was slightly negative in treatments where no

alkalinity source was added to the incubated sand samples. The two-way ANOVA revealed significant

effects of sand, alkalinity source and their interaction on ΔpH_T ($p<0.05$).

η_{CO2} was prescribed to be 0.36 when sand without an anthropogenic alkalinity source was incubated

and 0.86 for olivine incubations (see section 2.6.). Calculated η_{CO2} for NaOH and slag treatments were

slightly lower due to relatively lower ΔAlkalinity in the presence of sand than without the presence of

sand (Fig 4C). Statistics are not provided for η_{CO2} data because assumptions of the ANOVA model

were heavily violated.
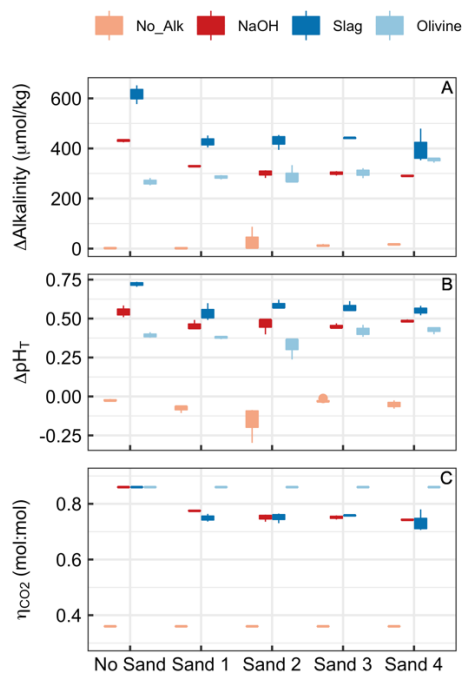
Figure 4. Results of Experiment 1. Changes of (A) alkalinity and (B) pH_T from the beginning to the

end of the 6.8 days experiment. (C) η_{CO2} at the end of the experiment. Boxplots are based on three

replicates per treatment. Colours refer to the added alkalinity source (No_Alk means no alkalinity

source was added). The alignment on the x-Axis indicates if (or which) sand sample was present in the

incubation bottles ("No Sand" means no Sand was added).

3.3. Experiment 2

The additions of CO_2-enriched seawater established a gradient of increasing DIC and accordingly a

decline in pH_T and Ω_{Arg} (Table S3). The rationale for this setup was that beach sediments can contain

high amounts of respiratory CO_2 so that anthropogenic alkalinity added to beaches has a high likelihood

to be exposed to such high CO_2 conditions (Liu et al., 2021; Perkins et al., 2022; Reckhardt et al., 2015).

Fig. 5 shows ΔAlkalinity along the DIC gradient for different alkalinity source materials (NaOH, slag,

olivine) and compares this to ΔAlkalinity along the same DIC gradient where only sand from a beach

was present. The "sand only" data is identical in all four plots (orange lines in Fig. 5). It shows that ΔAlkalinity is close to zero in the sand-only incubations when no DIC is added but increases exponentially with increasing DIC additions up to 537 µmol/kg.

OAE via NaOH additions was set up in two different scenarios (Fig. 5A, B). In the first scenario, the carbonate system was equilibrated with atmospheric CO_2 after the NaOH deployment and before exposed to the sand (Fig. 5A). Such a scenario could occur when NaOH is added to the ocean, but subsequent air-sea CO_2 influx fully equilibrated the NaOH-induced seawater CO_2 deficit before any interactions with sediments occur. Likewise, equilibration of CO_2-defficient seawater could be established within the electrochemical OAE facility and thus before the alkalinity-enhanced seawater is discharged back into the ocean. The equilibrated setup leads to a gradient in Ω_{Arg} from 2.1 to 0.2 at the beginning of the 6.8 days incubations (highest Ω_{Arg} at the lowest DIC addition). In the second scenario, the carbonate system was not equilibrated, thereby assuming that a NaOH-enriched patch of seawater would be exposed to sand sediments before it had taken up atmospheric CO_2 (Fig. 5B). Here, initial Ω_{Arg} ranges from 7.1 to 2.3 along the DIC gradient. In the equilibrated scenario, ΔAlkalinity was 482 µmol/kg when no DIC was added and increased exponentially to 973 µmol/kg at the highest DIC addition (Fig. 5A). In the unequilibrated scenario, ΔAlkalinity was 344 µmol/kg when no DIC was added and increased to 474 µmol/kg at the highest DIC addition. However, in contrast to the equilibrated treatment, the ΔAlkalinity increase in the unequilibrated treatment weakened along the DIC gradient and ΔAlkalinity was lower than in the sand-only treatment when the DIC addition was >400 µmol/kg (Fig. 5B).

In the slag treatment, ΔAlkalinity was 521 µmol/kg when no DIC was added. ΔAlkalinity increased exponentially along the DIC gradient to 814 µmol/kg. The increase of ΔAlkalinity was less pronounced than in the sand-only treatment. Overall, the slag data showed more scatter relative to the other alkalinity source materials and sand-only treatments (Fig. 5C).

In the olivine treatment, ΔAlkalinity was 258 µmol/kg when no DIC was added. ΔAlkalinity increased exponentially with increasing DIC additions to 453 µmol/kg although much less pronounced than in the sand-only treatment. ΔAlkalinity was lower in the olivine than in the sand-only treatment when DIC additions were >350 µmol/kg (Fig. 5C).

510
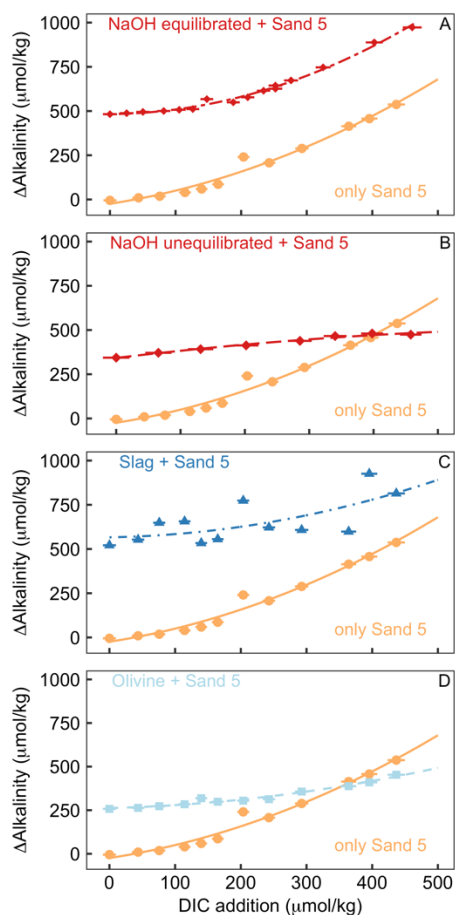
Figure 5. Results of Experiment 2. All panels show the change in alkalinity from the beginning to the end of the 6.8 days experiment along a gradient of DIC added to the incubation bottles (DIC values shown here refer to the values calculated from alkalinity and pH at the start of the experiment). The orange data displayed on all panels show ΔAlkalinity for incubations where only sand was incubated. The other data on each panel show ΔAlkalinity when sand was incubated with an external alkalinity source or addition scenario. Corresponding Ω_{Arg} and pH_T values for all scenarios are provided in Table S3. (A) Sand and NaOH equilibrated with atmospheric CO_2 upon addition; (B) Sand and NaOH which was not equilibrated with atmospheric CO_2 upon addition; (C) Sand and slag; (D) Sand and olivine.

3.4. Experiment 3

Experiment 3 tested if there is a carbonate chemistry dependency of alkalinity release by olivine and slag (Fig. 6). The two-way ANOVA revealed a significant influence of pH_T on the release of alkalinity from olivine and slag (Fig. 6, please note that pH_T was used for analysing the data but other carbonate chemistry parameters could also be the driver of the response). Slag released 707 ±61 µmol/kg alkalinity when incubated within a pH_T from initially 7.82 to 8.67 at the end of the 6.8 days incubation. Within the lower pH_T range from 6.86-8.39, slag released 805 ±86 µmol/kg. Olivine released 234 ±36 µmol/kg

when incubated within a pH_T from initially 7.82 to 8.20 at the end of the 6.8 days incubation. Within the lower low pH_T range from 6.86-7.63, olivine released 298 ±8 µmol/kg (Fig. 5).
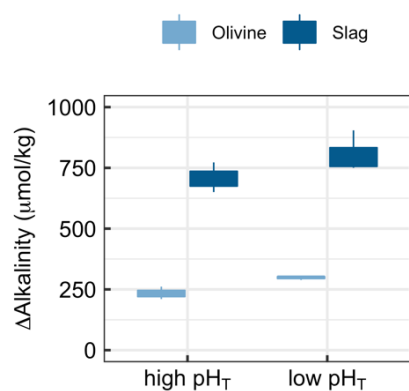
Figure 6. Results of Experiment 3. Changes in alkalinity from the beginning to the end of the 6.8 days experiment when olivine or slag were incubated (without sand) under high (initially 7.82) or low pH_T (initially 6.85). ΔAlkalinity was significantly higher under low pH_T ($p<0.05$).

4. Discussion

4.1. Carbonate-derived alkalinity is less efficient for CDR than non-carbonate-derived alkalinity

Section 2.6. introduced equations which show that alkalinity originating from carbonates ($Alk_{carbonate}$) has considerably less capacity to absorb CO_2 than alkalinity originating from non-carbonate sources such as olivine, slag, or NaOH ($Alk_{non-carbonate}$). The large influence of this chemical constraint on OAE is exemplified in Fig. 7. Here, the uptake potential for atmospheric CO_2 per mol alkalinity added to the ocean (η_{CO2}) is shown as a function of the carbonate contribution to the alkalinity source. When all ΔAlkalinity delivered via OAE originates from non-carbonate sources (e.g., NaOH, slag, olivine), then η_{CO2} equals 0.86. η_{CO2} declines linearly with an increasing contribution $Alk_{carbonate}$ to ΔAlkalinity to the lowest theoretical value for η_{CO2} of 0.36, which is reached when OAE provides all alkalinity as $Alk_{carbonate}$ (Fig. 7).

The dependency of η_{CO2} on the alkalinity source material (Fig. 7) has important implications for OAE methods that aim to utilise $CaCO_3$ as alkalinity source (Renforth et al., 2022; Wallmann et al., 2022; Harvey, 2008; Rau and Caldeira, 1999). The molar efficiency for atmospheric CO_2 sequestration of OAE is >50% lower when using carbonates (e.g. $CaCO_3$). Or put differently, OAE approaches utilising $CaCO_3$ as alkalinity source would have to increase alkalinity by more than twice as much to generate similar CDR compared to methods that use non-carbonates (e.g. NaOH, slag, or olivine). Importantly, while this disadvantage of carbonate sources of alkalinity appears to be substantial, it is not the only

557   important factor determining the potential of such OAE approaches. It is possible that the use of

558   carbonates still holds higher potential, for example because limestone is relatively abundant (Caserini

559   et al., 2022), can dissolve quickly (Renforth et al., 2022), or because it contains fewer components

560   potentially affecting marine organisms (Bach et al., 2019). Nevertheless, the dependency of η_{CO2} on the

561   alkalinity source (Fig. 7) needs to be considered when assessing the efficiency of different OAE

562   methods, as will become apparent in section 4.2.

563
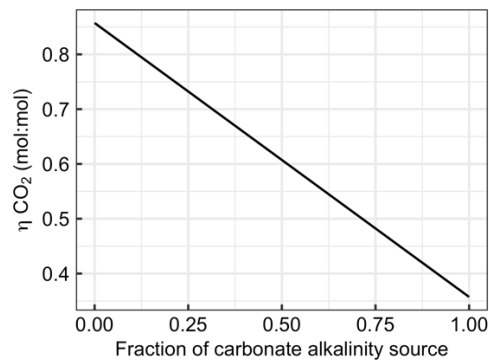
564

565   **Figure 7**. Changes in η_{CO2} with the fraction alkalinity originating from carbonates (e.g. $CaCO_3$

566   dissolution). The x-axis ranges from 0 (all ΔAlkalinity originates from non-carbonate sources such as

567   NaOH, slag, or olivine) to 1 (all ΔAlkalinity originates from carbonate sources such as $CaCO_3$ or

568     $MgCO_3$).

569

570   **4.2. The additionality problem of OAE**

571

572   The experiments considered here investigate coastal applications of OAE, for example when ground

573   materials or NaOH are exposed to beaches or sandy sediments. In the experiments, the treatments where

574   only sand was incubated constitute the baseline system while incubations of sand and an alkalinity

575   source constitute the OAE deployments. Both the baseline system and the OAE deployment were run

576   in parallel under identical conditions. To assess the additionality of OAE, CO_2 sequestration achieved

577   through an OAE deployment must be compared to the baseline state where no such deployment

578   occurred (see eq. 4). As such, additionality can be affected through processes that affect the OAE

579   deployment directly (section 4.2.1.), or when the OAE deployment alters the baseline state of the system

580   (section 4.2.2.).

581

582   **4.2.1.   Change of additionality through interaction of alkalinity sources with sand**

583

584   The ΔAlkalinities determined in Experiment 1 were lower in NaOH and slag incubations with sand than

585   in incubations without sand. The reduction in the presence of sand was likely due secondary

586   precipitation of carbonates, which is promoted when Ω_{CaCO3} is elevated and/or there are particles (here

587   sand), which provide nucleation sites for $CaCO_3$ precipitation (Moras et al., 2022; Fuhr et al., 2022;

588   Zhong and Mucci, 1989).

589   In contrast to the NaOH and slag incubations, the olivine incubations generated more ΔAlkalinity when

590   sand was present, even though the enhancement was small and only in one case statistically significant

591   (i.e., No Sand vs Sand 4; Fig. 4A). This contrasting observation can be explained as follows. First,

592   ΔAlkalinity was generally lower in the olivine incubations than in the NaOH and slag incubations when

593   no sand was present (266 ±14.8 µmol/kg for olivine vs. >420 µmol/kg for NaOH and slag). Moras et

594   al., (2022) have shown that the onset of secondary precipitation depends on ΔAlkalinity and they

595   observed no secondary precipitation over a 40-day experimental incubation when ΔAlkalinity was ~250

596   µmol/kg (Ω_{Arg}=~4). This suggests that the 266 ±14.8 µmol/kg ΔAlkalinity generated by olivine did not

597   elevate Ω_{Arg} to high enough levels to induce noticeable secondary precipitation within 6.8 days.

598   However, the absence of such secondary precipitation cannot explain why ΔAlkalinity increased in the

599   presence of sand. It is possible that the sand itself released alkalinity via carbonate dissolution as a very

600   small increase in ΔAlkalinity was also observed in some sand-only incubations (e.g. 17.4 ±2.6 µmol/kg

601   in Sand 4; Fig. 4A). However, Ω_{Arg} was higher in the olivine incubations as in the sand-only treatment

602   so that a release of carbonate alkalinity seems unlikely. It is also unlikely that the pH differences

603   between olivine-only and olivine+sand incubations drove this trend. While Experiment 3 underscores

604   that lower pH promotes the release of alkalinity from olivine (Fig. 6), pH_T was higher in the

605   olivine+sand treatment where significantly more alkalinity was released (see Sand 4 in Fig. 5A). What

606   appears as a plausible explanation is that the sand caused physical destruction of coatings that develop

607   on the olivine particles during dissolution and are known to reduce dissolution rates (Oelkers et al.,

608   2018). Indeed, the dissolution-enhancing role physical abrasion has been hypothesised to increase OAE

609   efficiency when using olivine (Schuiling and de Boer, 2010), as has recently been confirmed by

610   (Flipkens et al., 2023).

611   η_{CO2} is reduced when the presence of sand catalyses secondary precipitation (Fig. 5C). Consequently,

612   the amount of DIC that can be sequestered via OAE declines. Among other factors, the degree of

613   alkalinity loss due to secondary precipitation depends on the duration carbonate supersaturated water is

614   exposed to the sand. The experiments presented here lasted for 6.8 days and it is likely that secondary

615   precipitation would have proceeded (and η_{CO2} further declined) if the experiments had lasted for longer.

616   Indeed, Moras et al., (2022) observed that secondary precipitation catalysed by particles only slowed

617   down once Ω_{Arg} reached ~2. In the experiments presented here, Ω_{Arg} was generally >5 at the end of the

618   study. A back-of-the-envelope carbonate chemistry calculation with seacarb suggests that a decline until

619   Ω_{Arg} reaches 2 via carbonate precipitation (i.e. alkalinity and DIC decline in a 2:1 molar ratio) would

620   have reduced alkalinity by ~560 µmol/kg for the NaOH and 840 µmol/kg for the slag incubations,

621   respectively. In both cases the alkalinity after the OAE perturbation would be lower than before but

622 atmospheric CO_2 uptake would still occur (η_{CO2} = 0.39 for NaOH and 0.37 for slag) because the pCO_2

623 is still slightly lower than before the perturbation (Moras et al., 2022).

624

625 ### 4.2.2. Reduction of additionality through modification of baseline alkalinity
626 ### formation

627

628 One interesting observation was made during a sand-only incubation of Experiment 1 (i.e. "No_Alk in

629 Fig. 4). For Sand 2, ΔAlkalinity was about 85 µmol/kg higher in one replicate bottle than in the other

630 two. This difference was due to a small arthropod (likely a sand flea) that was unintentionally added to

631 the incubation bottle where the high ΔAlkalinity was observed. The arthropod was still alive at the end

632 of the 6.8 incubation period. During those 6.8 days, the organism respired, thereby reducing Ω_{Arg}, and

633 causing alkalinity release from the sand via $CaCO_3$ dissolution. This observation pointed out that the

634 baseline system can already release substantial amounts of alkalinity even before OAE is implemented

635 given sufficient respiration. Indeed, the in-situ observations at Clifton South suggest that alkalinity

636 release occurs in the baseline system used here (section 3.1). Furthermore, there is widespread evidence

637 from the literature that beaches release alkalinity via $CaCO_3$ dissolution (Liu et al., 2021; Perkins et al.,

638 2022; Reckhardt et al., 2015). These insights collectively inspired Experiment 2, where a DIC gradient

639 (high to low Ω_{Arg}) was set up to test if natural alkalinity release via $CaCO_3$ dissolution would be

640 influenced by anthropogenic alkalinity release via OAE.

641 Experiment 2 demonstrated that the release of natural alkalinity can be disturbed by the addition of

642 anthropogenic alkalinity sources (Fig. 8). Fig. 8A illustrates the additionality of alkalinity release,

643 calculated by subtracting ΔAlkalinity from sand-only incubations (represented by the orange lines in

644 Fig. 5 panels A-D) from ΔAlkalinity in sand+alkalinity incubations (represented by the red and blue

645 lines). Fig. 8A reveals that the additionality of ΔAlkalinity declines with increasing amounts of added

646 DIC. The reason for this trend is that the alkalinity sources added to the incubation bottles buffered the

647 DIC-induced pH decline. This buffering elevated Ω_{Arg} during the incubations, resulting in a reduced

648 release of natural alkalinity through $CaCO_3$ dissolution. Or in simpler terms, by adding a new buffer

649 system via OAE (NaOH, slag, or olivine), a natural buffer system ($CaCO_3$ dissolution) is partially

650 replaced. In cases where olivine or non-equilibrated NaOH was tested, the additionality of ΔAlkalinity

651 became even negative when DIC additions were >350 and >400 µmol/kg, respectively (Fig. 8A).

652 Alkalinity release is generally seen as a good indicator for the amount of CO_2 that can be removed per

653 mole alkalinity enhancement (η_{CO2}). However, as discussed in section 4.1., η_{CO2} also critically depends

654 on whether the released alkalinity is $Alk_{carbonate}$ or $Alk_{non-carbonate}$. In Experiment 2, η_{CO2} varies greatly

655 depending on the alkalinity source and the amount of DIC added to the incubation (Fig. 8B). η_{CO2} is

656 low for sand-only incubations because basically all ΔAlkalinity is $Alk_{carbonate}$, whereas it is substantially

657 higher in treatments with an anthropogenic $Alk_{non-carbonate}$ source. For olivine, η_{CO2} was around 0.7 up

658   until the highest DIC additions where η_{CO2} declines slightly. This is lower than for slag, where η_{CO2}

659   remains close to the theoretical maximum of 0.86. The difference between slag and olivine could be

660   due to faster dissolution of slag, which elevates Ω_{Arg} before substantial $CaCO_3$ dissolution had occurred.

661   In contrast, olivine dissolves more slowly (Fuhr et al., 2022; Montserrat et al., 2017; Hangx and Spiers,

662   2009), so that some $CaCO_3$ dissolution may have occurred before olivine dissolution elevated Ω_{Arg}

663   enough to limit further $CaCO_3$ dissolution. (Please note, however, that this explanation does not explain

664   why η_{CO2} is also lower than in slag incubations at low DIC additions, where Ω_{Arg} was high enough to

665   limit $CaCO_3$ dissolution from the start). The reason for the decreasing η_{CO2} in the equilibrated NaOH

666   scenario (Fig. 8B) is an increasing contribution of $Alk_{carbonate}$ to ΔAlkalinity. It is important to note that

667   for the same added DIC, Ω_{Arg} is much lower in the equilibrated NaOH scenario than in unequilibrated

668   NaOH scenario (e.g. 0.28 vs. 2.9 at ~400 µmol/kg added DIC for the equilibrated and unequilibrated

669   NaOH scenarios, respectively). This lower Ω_{Arg} is because the equilibrated scenario simulates that

670   atmospheric CO_2 has already been absorbed by the alkalinity-enhanced seawater. Accordingly,

671   alkalinity-enhanced seawater that has been equilibrated with atmospheric CO_2 interacts with beach

672   sediments at a lower Ω_{Arg} than if the alkalinity-enhanced seawater was unequilibrated. As such, the

673   equilibrated OAE scenario causes less reduction of natural alkalinity release from sediments via $CaCO_3$

674   dissolution.

675   Measurements and estimates of ΔAlkalinity and η_{CO2} enabled calculation of how much DIC could be

676   maximally stored by the generated alkalinity (i.e., DIC_{OAE} as calculated in eq. 9 is shown in Fig. 8C).

677   DIC_{OAE} increases with higher DIC additions due to the release of alkalinity via $CaCO_3$ dissolution.

678   However, the increase is less pronounced as observed for ΔAlkalinity (Fig. 8A) because $Alk_{carbonate}$ from

679    $CaCO_3$ dissolution is less efficient in sequestering environmental CO_2 than $Alk_{non-carbonate}$ from NaOH,

680   slag, or olivine (section 4.1).

681   To calculate the additionality of DIC_{OAE}, I subtracted DIC_{OAE} of the sand-only incubations (baseline)

682   of DIC_{OAE} of the OAE scenarios (Fig. 8D). The additionality of DIC_{OAE} is arguably the most important

683   parameter to assess whether an OAE deployment has led to the net sequestration of CO_2. In the case of

684   the equilibrated NaOH and slag scenarios, the additionality of DIC_{OAE} was constant over the applied

685   gradient, suggesting that the release of $Alk_{carbonate}$ via $CaCO_3$ dissolution led to similar DIC_{OAE} potential

686   in the sand-only scenario and these two OAE scenarios. In contrast, the additionality of DIC_{OAE} declined

687   in the olivine scenario because there was relatively more $Alk_{carbonate}$ release in the sand only scenario

688   than in the olivine scenario (Fig. 8D). Importantly, however, the additionality of DIC_{OAE} remains

689   positive up until the highest DIC addition, which is in stark contrast to the additionality of ΔAlkalinity

690   (compare Fig 8A and D). This means that the addition of olivine maintained a positive CO_2

691   sequestration potential even though less alkalinity was generated in the olivine treatment than in the

692   sand-only treatment (Fig. 8C). The reason for this counterintuitive observation is simply that the Alk_{non-}

693 _{carbonate} released by olivine has more potential to sequester CO_2 than the $Alk_{carbonate}$ released via $CaCO_3$

694 dissolution.

695
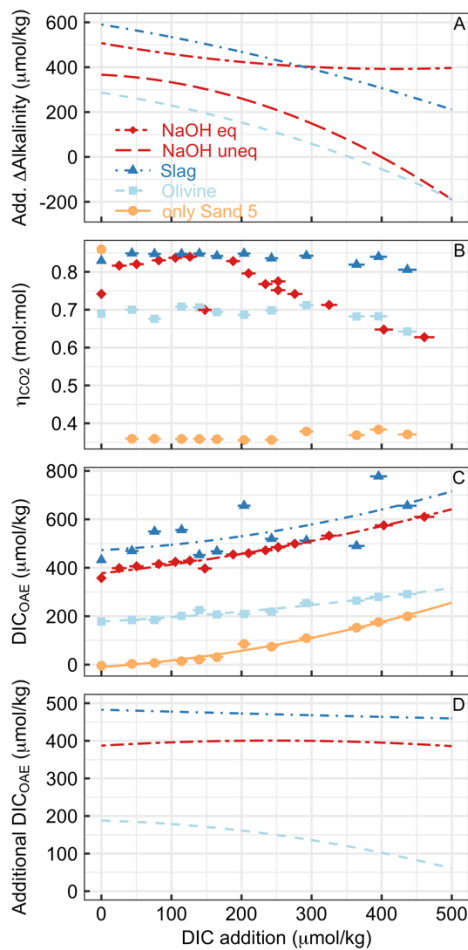
696

697 **Figure 8**. Various measures of OAE efficiency under increasing additions of DIC in Experiment 2 (DIC

698 could for example be CO_2 from the respiration of organic material in sediments). (A) The additionality

699 of ΔAlkalinity. (B) η_{CO2} at the end of the experiment. Please note that the extreme outlier at lowest DIC

700 addition in the sand-only treatment was likely due to measurement uncertainty. (C) DIC_{OAE}, i.e., how

701 much seawater CO_2 could have potentially been absorbed with the amount of ΔAlkalinity provided by

702 the various alkalinity sources. (D) The additionality of DIC_{OAE}. Please note that panels (B-D) only show

703 data for the equilibrated NaOH scenario. I omitted the unequilibrated scenario for logical reasons, i.e.,

704 because the core assumption in this scenario (no CO_2 equilibration with the atmosphere after OAE) is

705 at odds with the necessary assumption of CO_2 equilibration to calculate η_{CO2} (section 2.6).

706

707 **4.3. Relevance of the additionality problem**

708

709 Modifications of additionality can occur when OAE triggers subsequent alkalinity loss through biotic

710 and abiotic carbonate precipitation (section 4.2.1.). This feedback has been widely discussed and is

already a predominant topic in OAE research (Hartmann et al., 2013; Bach et al., 2019; Moras et al., 2022; Fuhr et al., 2022; Hartmann et al., 2023). Not yet discussed is the modification of additionality that may occur when anthropogenic alkalinity sources (via OAE) modify the release of natural alkalinity (section 4.2.2.). Thus, I will focus on the relevance of this second pathway of additionality modification in the following paragraphs.

The experiments conducted here tested how anthropogenic alkalinity sources can interact with beach sand in a setting that assumes constant mixing, inspired by conditions observed in a high energy wave impact zone. This setting was chosen based on the widely discussed OAE implementation strategy of adding olivine powder to beaches. The results suggest that the "additionality problem" needs to be considered for this specific OAE approach. However, the wave impact zone comprises a tiny fraction of the coastal ocean and the question is to what extent the additionality problem also applies to the vast shelf, bank, embayment and reef areas where OAE could also be implemented (Feng et al., 2017; Meysman and Montserrat, 2017; Mongin et al., 2021).

The coastal ocean is a net sink of ~ 36 Tmol/year alkalinity via $CaCO_3$ burial (Middelburg et al., 2020), but considerable amounts of alkalinity are also generated in the various coastal sediments via $CaCO_3$ dissolution (one estimate suggests ~13 Tmol/year; (Krumins et al., 2013)). The dissolution depends on the solubility of $CaCO_3$ present in the sediments and pore water Ω_{CaCO3} (Middelburg et al., 2020). Conditions for dissolution are generally favourable in coastal ocean sediments because soluble forms of $CaCO_3$ occur more frequently and relatively high supply of organic matter lowers Ω_{CaCO3} (Krumins et al., 2013; Lunstrum and Berelson, 2022; Morse et al., 1985). Thus, the introduction of an anthropogenic buffer via OAE (which increases Ω_{CaCO3}) is likely to cause a reduction of alkalinity release from the seafloor.

Indeed, more soluble forms of $CaCO_3$ were shown to protect less soluble forms of $CaCO_3$ from dissolution at the seafloor (Sulpis et al., 2022). Furthermore, an experiment exposed a coral reef to moderate levels of increased alkalinity (ΔAlkalinity = ~50 µmol/kg) and found a net increase of reef calcification, with some evidence suggesting that the measured effect was due to reduced reef dissolution (Albright et al., 2016). Anthropogenic alkalinity sources (e.g. NaOH, slag, olivine) introduced via OAE can be considered to have a similar effect and reduce natural alkalinity release via $CaCO_3$ dissolution. It is worth noting that the negative effect of anthropogenic alkalinity on natural alkalinity release may also occur in the open surface ocean. Here, part of the alkalinity bound in particulate form via biotic calcification re-dissolves, for example in corrosive microenvironments such as zooplankton or marine snow (Subhas et al., 2022; Milliman et al., 1999; Sulpis et al., 2021). If anthropogenic alkalinity introduced via OAE reduces this natural dissolution of $CaCO_3$ in the surface ocean, then less alkalinity would remain in the surface ocean and the additionality of OAE would be reduced (Bach et al., 2019). Thus, the "additionality problem" of OAE could be widespread and not restricted to the specific environment studied experimentally in this paper.

747   Another interesting aspect to consider is the time and scale-dependency of the additionality
748   problem. A detectable slow-down of natural alkalinity formation may occur in the environment where
749   anthropogenic alkalinity was added (as observed in the experiments presented here). Such an "acute"
750   additionality problem may be comparatively easy to associate with the responsible OAE deployment
751   and there may be straight-forward ways to mitigate it. (see section 4.4 and Box 1). However, the
752   problem could turn from "acute" to "chronic" over much longer timescales should OAE be up-scaled
753   to climate-relevance and cause a significant increase of Ω throughout the ocean. In the chronic scenario,
754   anthropogenic alkalinity may partially replace the "natural" alkalinity release enforced by fossil fuel
755   CO_2 neutralization via carbonate dissolution (Archer et al., 1998). A chronic additionality problem
756   would unlikely be attributable to individual OAE deployments and suggested mitigation measures
757   described in section 4.4. and Box 1 would not work. Indeed, similar chronic problems for CDR imposed
758   by Earth system feedbacks have already been described, for example the possible weakening of natural
759   terrestrial and marine CO_2 sinks due to CDR implementation (Keller et al., 2018). However, assessing
760   whether the hypothesis of a chronic additionality problem is valid remains to be seen and will require
761   more targeted follow-up research.
762
763   ### 4.4. Possible ways to manage the additionality problem
764
765   This section discusses potential pathways to manage an acute additionality problem. The discussion is
766   accompanied with Box 1, which translates thoughts raised here into suggestions how practitioners (e.g.
767   OAE start-ups) could deal with acute additionality problems.
768   To manage the additionality problem, it is important to monitor the natural alkalinity release in a
769   designated OAE deployment site before OAE is implemented. Natural alkalinity release occurs in all
770   coastal habitats (Krumins et al., 2013; Aller, 1982; Perkins et al., 2022; Liu et al., 2021) and recent
771   evidence suggests that even small $CaCO_3$ content in sediments is sufficient to yield high alkalinity
772   release rates (Lunstrum and Berelson, 2022). As such, dissolution is not restricted to $CaCO_3$ rich
773   sediments and avoiding these may therefore not mitigate the additionality problem. More crucial than
774   the $CaCO_3$ content appears to be the supply of organic matter to the seafloor, which provides respiratory
775   CO_2 needed for $CaCO_3$ dissolution and associated alkalinity release (but note that organic matter supply
776   also drives organic or other inorganic alkalinity release (Krumins et al., 2013; Aller, 1982; Lunstrum
777   and Berelson, 2022; Perkins et al., 2022; Liu et al., 2021)). Therefore, it may be useful to avoid OAE
778   near sediments exposed to high organic matter load to reduce the interference of anthropogenic
779   alkalinity with natural alkalinity release.
780   Another mitigation pathway for the additionality problem is dilution. When anthropogenic alkalinity is
781   diluted quickly then there is less chance for the new buffer system to generate oversaturated Ω in
782   seawater, sediment pore waters, or other microenvironments. Indeed, the data from the beach transects
783   show that alkalinity (and $Si(OH)_4$) deviations in the upper end of the swash zone were quickly lost upon

moving offshore (Fig. 3). The experiments presented here do not allow for such dilution as they are performed in enclosed volumes. They can therefore be considered a more extreme case, which do not correctly represent the vastness of the ocean and its volume. Indeed, previous experiments investigating the risk of alkalinity loss after OAE due to secondary precipitation found that dilution effectively mitigates the secondary precipitation problem (Moras et al., 2022). It is very likely that dilution is similarly effective to mitigate the additionality problem.

Finally, the data presented here clearly show that the additionality problem scales with the degree of $CaCO_3$ oversaturation introduced through the anthropogenic alkalinity source. This is most obvious when comparing the equilibrated with the unequilibrated NaOH OAE scenario. The increase of Ω_{CaCO3} is much more pronounced in the unequilibrated scenario because atmospheric CO_2 has not yet entered the seawater and brought down Ω_{CaCO3} to levels it was before the OAE perturbation. As such, the additionality problem will be much more pronounced when an alkalinity source interacts with naturally alkalinity releasing sediments before the OAE-perturbed seawater has been equilibrated with atmospheric CO_2. Nevertheless, a close look at Fig. 4A (equilibrated NaOH) shows that even the relatively small increase of Ω_{CaCO3} that coincides with OAE fully equilibrated with atmospheric CO_2, can reduce natural alkalinity release. Thus, atmospheric CO_2 equilibration following OAE mitigates the additionality problem but cannot fully avoid it.

Box 1. Suggestions for OAE practitioners.

Research much beyond the present study is needed to better constrain the magnitude of the additionality problem and evaluate its relevance for OAE. However, real-world OAE assessments and ambitions for implementation are already underway so that some initial guidance on the additionality problem may be important already now, even if based on limited evidence. This Box translates thoughts discussed in section 4 into suggestions directed to those working on the implementation of OAE. Importantly, practitioners should remain critical about these suggestions (they may change with further knowledge gain) and apply at own risk.

- With the currently limited understanding of the additionality problem, it may be best to avoid it as much as possible.
- Choose a field site with high dilution. Interaction of anthropogenic alkalinity with the natural alkalinity cycle are less likely to occur when alkalinity-enhanced seawater is quickly mixed with unperturbed seawater. As such, volumes with restricted exchange (e.g. bays, lagoons, fjords) may be more problematic.
- Enable fast equilibration of the alkalinity-enhanced seawater with atmospheric CO_2. The influx of atmospheric CO_2 returns Ω_{CaCO3} of alkalinity-enhanced seawater to values closer to unperturbed seawater and thus has less potential to affect $CaCO_3$ dissolution or precipitation.

821   -   When possible, restrict contact of anthropogenic alkalinity with sediments to reduce
822   interactions at hotspots of natural alkalinity cycling. This suggestion is not feasible for OAE
823   implementation via coastal enhanced weathering where alkaline minerals are added to
824   sediments (Eisaman et al., 2023). For this OAE strategy, it is suggested to prefer sediments
825   depleted in organic matter where less "fuel" is available for respiration and associated carbonate
826   dissolution (i.e., natural alkalinity release).
827   -   Frameworks to monitor, report, and verify the success of OAE should include sediment
828   interactions and account for the additionality problem.

829

5. Conclusion and outlook

831

The additionality problem described herein could influence the effectiveness of OAE. It suggests that interference of anthropogenic alkalinity with the natural alkalinity cycle must be assessed as a factor that can modify the OAE efficiency. The arguments provided in the discussion suggest that the additionality problem is potentially widespread, even though the dataset presented here only considers OAE near or on wave-exposed beaches. Future research should aim to confirm or dismiss these arguments and to better understand the extent of the problem.

The additionality problem adds a layer of complexity to monitoring, reporting, and verification of CO_2 removal with OAE. Strictly speaking, it is not sufficient to monitor the generation (e.g., via NaOH, slag, or olivine dissolution) and potential loss (e.g., via biotic and abiotic precipitation) of anthropogenic alkalinity after its generation. It also needs to be assessed to what extent anthropogenic alkalinity alters the baseline removal or delivery of natural alkalinity. It will be crucial to understand whether the anthropogenic acceleration of the alkalinity cycle in the oceans via OAE could slow down the natural alkalinity cycle.

Competing interests

The author declares no competing interests.

Acknowledgements

I thank Jiaying Guo and Bec Lenc for providing particle size spectra, the Moyne Shire Council for providing olivine samples, Bradley Mansell from Liberty Primary Steel for providing steel slag aggregates, and the Central Science Laboratory at the University of Tasmania for particulate carbon analyses. I also Jack Middelburg for editing the manuscript and Matt Eisaman, Adam Subhas, and two anonymous reviewers for their constructive review. This research was funded through a Future Fellowship Award by the Australian Research Council (FT200100846) and by the Carbon-to-Sea Initiative, a non-profit dedicated to evaluating Ocean Alkalinity Enhancement.

858 **Data availability statement**

859 All data and evaluation scripts (for R) generated herein are available for download at zenodo.org under

860 the doi:10.5281/zenodo.8191516.

861

862 **Author contributions**

863 LTB conceived and performed the research and wrote the paper.

864

865 **References**

866 Adkins, J. F., Naviaux, J. D., Subhas, A. V, Dong, S., and Berelson, W. M.: The Dissolution Rate
867 of CaCO3 in the Ocean, https://doi.org/10.1146/annurev-marine-041720, 2020.
868 Albright, R., Caldeira, L., Hosfelt, J., Kwiatkowski, L., Maclaren, J. K., Mason, B. M.,
869 Nebuchina, Y., Ninokawa, A., Pongratz, J., Ricke, K. L., Rivlin, T., Schneider, K., Sesboüé, M.,
870 Shamberger, K., Silverman, J., Wolfe, K., Zhu, K., and Caldeira, K.: Reversal of ocean
871 acidification enhances net coral reef calcification, Nature, 531, 362–365,
872 https://doi.org/10.1038/nature17155, 2016.
873 Aller, R. C.: Carbonate Dissolution in Nearshore Terrigenous Muds: The Role of Physical and
874 Biological Reworking, J Geol, 90, 79–95, https://doi.org/10.1086/628652, 1982.
875 Archer, D., Kheshgi, H., and Maier-Reimer, E.: Dynamics of fossil fuel CO2 neutralization by
876 marine CaCO3, Global Biogeochem Cycles, 12, 259–276,
877 https://doi.org/10.1029/98GB00744, 1998.
878 Bach, L. T., Gill, S. J., Rickaby, R. E. M., Gore, S., and Renforth, P.: CO2 Removal With
879 Enhanced Weathering and Ocean Alkalinity Enhancement: Potential Risks and Co-benefits
880 for Marine Pelagic Ecosystems, Frontiers in Climate, 1, 1–21,
881 https://doi.org/10.3389/fclim.2019.00007, 2019.
882 Caserini, S., Storni, N., and Grosso, M.: The Availability of Limestone and Other Raw
883 Materials for Ocean Alkalinity Enhancement, Global Biogeochem Cycles, 36,
884 https://doi.org/10.1029/2021GB007246, 2022.
885 Dickson, A. G., Afghan, J. D., and Anderson, G. C.: Reference materials for oceanic CO2
886 analysis: a method for the certification of total alkalinity, Mar Chem, 80, 185–197,
887 https://doi.org/10.1016/S0304-4203(02)00133-0, 2003.
888 Dickson, A. G., Sabine, C. L., and Christian, J. R.: Guide to Best Practices for Ocean CO2
889 Measurements, PICES Spec., PICES, Sidney, 2007.
890 Eisaman, M. D., Rivest, J. L. B., Karnitz, S. D., Lannoy, C. De, Jose, A., Devaul, R. W., and
891 Hannun, K.: International Journal of Greenhouse Gas Control Indirect ocean capture of
892 atmospheric CO2 : Part II . Understanding the cost of negative emissions, International
893 Journal of Greenhouse Gas Control, 70, 254–261,
894 https://doi.org/10.1016/j.ijggc.2018.02.020, 2018.
895 Eisaman, M. D., Geilert, S., Renforth, P., Bastianini, L., Campbell, J., Dale, A. W., Foteinis, S.,
896 Grasse, P., Hawrot, O., Löscher, C. R., Rau, G. H., and Rønning, J.: Chapter 3: Assessing the
897 technical aspects of OAE approaches, in: Guide for best practices in Ocean Alkalinity
898 Enhancement, 2023.
899 Fakhraee, M., Planavsky, N. J., and Reinhard, C. T.: Ocean alkalinity enhancement through
900 restoration of blue carbon ecosystems, Nat Sustain, https://doi.org/10.1038/s41893-023-
901 01128-2, 2023.

902 Feng, E. Y., Koeve, W., Keller, D. P., and Oschlies, A.: Model-Based Assessment of the CO2
903 Sequestration Potential of Coastal Ocean Alkalinization, Earths Future, 5, 1252–1266,
904 https://doi.org/10.1002/eft2.273, 2017.

905 Ferderer, A., Chase, Z., Kennedy, F., Schulz, K. G., and Bach, L. T.: Assessing the influence of
906 ocean alkalinity enhancement on a coastal phytoplankton community, Biogeosciences, 19,
907 5375–5399, https://doi.org/10.5194/bg-19-5375-2022, 2022.

908 Flipkens, G., Fuhr, M., Meysman, F. J. R., Town, R. M., and Blust, R.: Enhanced olivine
909 dissolution in seawater through continuous grain collisions, Geochim Cosmochim Acta, 359,
910 84–99, https://doi.org/10.1016/j.gca.2023.09.002, 2023.

911 Fuhr, M., Geilert, S., Schmidt, M., Liebetrau, V., Vogt, C., Ledwig, B., and Wallmann, K.:
912 Kinetics of Olivine Weathering in Seawater: An Experimental Study, Frontiers in Climate, 4,
913 1–20, https://doi.org/10.3389/fclim.2022.831587, 2022.

914 Gattuso, J.-P., Epitalon, J.-M., Lavigne, H., and Orr, J.: Seacarb: seawater carbonate
915 chemistry with R. R package version 3.0, 2021.

916 Hangx, S. J. T. and Spiers, C. J.: Coastal spreading of olivine to control atmospheric CO2
917 concentrations: A critical analysis of viability, International Journal of Greenhouse Gas
918 Control, 3, 757–767, https://doi.org/10.1016/j.ijggc.2009.07.001, 2009.

919 Hansen, H. P. and Koroleff, F.: Determination of nutrients, in: Methods of Seawater Analysis,
920 edited by: Grasshoff, K., Kremling, K., and Ehrhardt, M., Wiley-VCH, Weinheim, 159–226,
921 1999.

922 Hartmann, J., West, A. J., Renforth, P., Köhler, P., de la Rocha, C., Wolf-Gladrow, D., Dürr, H.
923 H., and Scheffran, J.: Enhanced chemical weathering as a geoengineering strategy to reduce
924 atmospheric carbon dioxide, supply nutrients, and mitigate ocean acidification, Reviews of
925 Geophysics, 51, 113–149, https://doi.org/10.1002/rog.20004.1.Institute, 2013.

926 Hartmann, J., Suitner, N., Lim, C., Schneider, J., Marín-Samper, L., Arístegui, J., Renforth, P.,
927 Taucher, J., and Riebesell, U.: Stability of alkalinity in ocean alkalinity enhancement (OAE)
928 approaches - consequences for durability of CO2 storage, Biogeosciences, 20, 781–802,
929 https://doi.org/10.5194/bg-20-781-2023, 2023.

930 Harvey, L. D. D.: Mitigating the atmospheric CO2 increase and ocean acidification by adding
931 limestone powder to upwelling regions, J Geophys Res Oceans, 113, 1–21,
932 https://doi.org/10.1029/2007JC004373, 2008.

933 Havukainen, M., Waldén, P., and Kahiluoto, H.: Clean Development Mechanism, in:
934 Encyclopedia of Sustainable Management, edited by: Idowu, S. O., Springer Nature
935 Switzerland, 1–5, https://doi.org/10.1016/B978-0-12-375067-9.00127-3, 2022.

936 He, J. and Tyka, M. D.: Limits and CO2 equilibration of near-coast alkalinity enhancement,
937 Biogeosciences, 20, 27–43, https://doi.org/10.5194/bg-20-27-2023, 2023.

938 Humphreys, M. P., Gregor, L., Pierrot, D., van Heuven, S. M. A. C., Lewis, E. R., and Wallace,
939 D. W. R.: PyCO2SYS: marine carbonate system calculations in Python,
940 https://doi.org/10.5281/zenodo.3744275, 2020.

941 Keller, D. P., Lenton, A., Littleton, E. W., Oschlies, A., Scott, V., and Vaughan, N. E.: The
942 Effects of Carbon Dioxide Removal on the Carbon Cycle, Curr Clim Change Rep, 4, 250–265,
943 https://doi.org/10.1007/s40641-018-0104-3, 2018.

944 Krumins, V., Gehlen, M., Arndt, S., Van Cappellen, P., and Regnier, P.: Dissolved inorganic
945 carbon and alkalinity fluxes from coastal marine sediments: Model estimates for different
946 shelf environments and sensitivity to global change, Biogeosciences, 10, 371–398,
947 https://doi.org/10.5194/bg-10-371-2013, 2013.

948 de Lannoy, C. F., Eisaman, M. D., Jose, A., Karnitz, S. D., DeVaul, R. W., Hannun, K., and
949 Rivest, J. L. B.: Indirect ocean capture of atmospheric CO2: Part I. Prototype of a negative
950 emissions technology, International Journal of Greenhouse Gas Control, 70, 243–253,
951 https://doi.org/10.1016/j.ijggc.2017.10.007, 2018.
952 Lewis, E. L. and Perkin, R. G.: Salinity: Its definition and calculation, J Geophys Res Oceans,
953 83, 466–478, https://doi.org/10.1029/jc083ic01p00466, 1978.
954 Lezaun, J.: Hugging the Shore: Tackling Marine Carbon Dioxide Removal as a Local
955 Governance Problem, Frontiers in Climate, 3, 1–6,
956 https://doi.org/10.3389/fclim.2021.684063, 2021.
957 Liu, Y., Jiao, J. J., Liang, W., Santos, I. R., Kuang, X., and Robinson, C. E.: Inorganic carbon and
958 alkalinity biogeochemistry and fluxes in an intertidal beach aquifer: Implications for ocean
959 acidification, J Hydrol (Amst), 595, 126036, https://doi.org/10.1016/j.jhydrol.2021.126036,
960 2021.
961 Lueker, T. J., Dickson, A. G., and Keeling, C. D.: Ocean pCO2 calculated from dissolved
962 inorganic carbon, alkalinity, and equations for K1 and K2: Validation based on laboratory
963 measurements of CO2 in gas and seawater at equilibrium, Mar Chem, 70, 105–119,
964 https://doi.org/10.1016/S0304-4203(00)00022-0, 2000.
965 Lunstrum, A. and Berelson, W.: CaCO3 dissolution in carbonate-poor shelf sands increases
966 with ocean acidification and porewater residence time, Geochim Cosmochim Acta, 329,
967 168–184, https://doi.org/10.1016/j.gca.2022.04.031, 2022.
968 Meysman, F. J. R. and Montserrat, F.: Negative CO2 emissions via enhanced silicate
969 weathering in coastal environments, Biol Lett, 13, 20160905,
970 https://doi.org/10.1098/rsbl.2016.0905, 2017.
971 Michaelowa, A., Hermwille, L., Obergassel, W., and Butzengeiger, S.: Additionality revisited:
972 guarding the integrity of market mechanisms under the Paris Agreement, Climate Policy, 19,
973 1211–1224, https://doi.org/10.1080/14693062.2019.1628695, 2019.
974 Middelburg, J. J., Soetaert, K., and Hagens, M.: Ocean Alkalinity, Buffering and
975 Biogeochemical Processes, Reviews of Geophysics, 58,
976 https://doi.org/10.1029/2019RG000681, 2020.
977 Milliman, J. D., Troy, P. J., Balch, W. M., Adams, A. K., Li, Y.-H., and Mackenzie, F. T.:
978 Biologically mediated dissolution of calcium carbonate above the chemical lysocline?, Deep
979 Sea Research Part I: Oceanographic Research Papers, 46, 1653–1669,
980 https://doi.org/10.1016/S0967-0637(99)00034-5, 1999.
981 Mongin, M., Baird, M. E., Lenton, A., Neill, C., and Akl, J.: Reversing ocean acidification along
982 the Great Barrier Reef using alkalinity injection, Environmental Research Letters, 16,
983 https://doi.org/10.1088/1748-9326/ac002d, 2021.
984 Montserrat, F., Renforth, P., Hartmann, J., Leermakers, M., Knops, P., and Meysman, F. J. R.:
985 Olivine Dissolution in Seawater: Implications for CO2 Sequestration through Enhanced
986 Weathering in Coastal Environments, Environ Sci Technol, 51, 3960–3972,
987 https://doi.org/10.1021/acs.est.6b05942, 2017.
988 Moras, C. A., Bach, L. T., Cyronak, T., Joannes-Boyau, R., and Schulz, K. G.: Ocean alkalinity
989 enhancement - avoiding runaway CaCO3 precipitation during quick and hydrated lime
990 dissolution, Biogeosciences, 19, 3537–3557, https://doi.org/10.5194/bg-19-3537-2022,
991 2022.
992 Morse, J. W., Zullig, J. J., Bernstein, L. D., Millero, F. J., Milne, P., Mucci, A., and Choppin, G.
993 R.: Chemistry of calcium carbonate-rich shallow water sediments in the Bahamas., Am J Sci,
994 285, 147–185, https://doi.org/10.2475/ajs.285.2.147, 1985.

995   Morse, J. W., Gledhill, D. K., and Millero, F. J.: CaCO3 precipitation kinetics in waters from
996   the great Bahama bank: Implications for the relationship between bank hydrochemistry and
997   whitings, Geochim Cosmochim Acta, 67, 2819–2826, https://doi.org/10.1016/S0016-
998   7037(03)00103-0, 2003.
999   Mucci, A.: The solubility of calcite and aragonite in seawater at various salinities,
1000   temperatures, and one atmosphere total pressure, Am J Sci, 283, 780–799, 1983.
1001   Nemet, G. F., Callaghan, M. W., Creutzig, F., Fuss, S., Hartmann, J., Hilaire, J., Lamb, W. F.,
1002   Minx, J. C., Rogers, S., and Smith, P.: Negative emissions — Part 3: Innovation and upscaling,
1003   Environmental Research Letters, 13, 06300, 2018.
1004   Oelkers, E. H., Declercq, J., Saldi, G. D., Gislason, S. R., and Schott, J.: Olivine dissolution
1005   rates: A critical review, Chem Geol, 500, 1–19,
1006   https://doi.org/10.1016/j.chemgeo.2018.10.008, 2018.
1007   Perkins, A. K., Santos, I. R., Rose, A. L., Schulz, K. G., Grossart, H. P., Eyre, B. D., Kelaher, B. P.,
1008   and Oakes, J. M.: Production of dissolved carbon and alkalinity during macroalgal wrack
1009   degradation on beaches: a mesocosm experiment with implications for blue carbon,
1010   Biogeochemistry, 160, 159–175, https://doi.org/10.1007/s10533-022-00946-4, 2022.
1011   Rau, G. H. and Caldeira, K.: Enhanced carbonate dissolution: A means of sequestering waste
1012   CO2 as ocean bicarbonate, Energy Convers Manag, 40, 1803–1813,
1013   https://doi.org/10.1016/S0196-8904(99)00071-0, 1999.
1014   Reckhardt, A., Beck, M., Seidel, M., Riedel, T., Wehrmann, A., Bartholomä, A., Schnetger, B.,
1015   Dittmar, T., and Brumsack, H. J.: Carbon, nutrient and trace metal cycling in sandy
1016   sediments: Acomparison of high-energy beaches and backbarrier tidal flats, Estuar Coast
1017   Shelf Sci, 159, 1–14, https://doi.org/10.1016/j.ecss.2015.03.025, 2015.
1018   Renforth, P.: The negative emission potential of alkaline materials, Nat Commun, 10,
1019   https://doi.org/10.1038/s41467-019-09475-5, 2019.
1020   Renforth, P. and Henderson, G.: Assessing ocean alkalinity for carbon sequestration,
1021   Reviews of Geophysics, 55, 636–674, https://doi.org/10.1002/2016RG000533, 2017.
1022   Renforth, P., Baltruschat, S., Peterson, K., Mihailova, B. D., and Hartmann, J.: Using ikaite
1023   and other hydrated carbonate minerals to increase ocean alkalinity for carbon dioxide
1024   removal and environmental remediation, Joule, 6, 2674–2679,
1025   https://doi.org/10.1016/j.joule.2022.11.001, 2022.
1026   Saderne, V., Fusi, M., Thomson, T., Dunne, A., Mahmud, F., Roth, F., Carvalho, S., and
1027   Duarte, C. M.: Total alkalinity production in a mangrove ecosystem reveals an overlooked
1028   Blue Carbon component, Limnol Oceanogr Lett, 6, 61–67,
1029   https://doi.org/10.1002/lol2.10170, 2021.
1030   Schuiling, R. D. and de Boer, P. L.: Coastal spreading of olivine to control atmospheric CO2
1031   concentrations: A critical analysis of viability. Comment: Nature and laboratory models are
1032   different, International Journal of Greenhouse Gas Control, 4, 855–856,
1033   https://doi.org/10.1016/j.ijggc.2010.04.012, 2010.
1034   Schuiling, R. D. and Krijgsman, P.: Enhanced weathering: An effective and cheap tool to
1035   sequester CO2, Clim Change, 74, 349–354, https://doi.org/10.1007/s10584-005-3485-y,
1036   2006.
1037   Schulz, K. G., Bach, L. T., and Dickson, A. G.: Seawater carbonate system considerations for
1038   ocean alkalinity enhancement research, Guide for best practices in Ocean Alkalinity
1039   Enhancement, 2023.
1040   Subhas, A. V., Dong, S., Naviaux, J. D., Rollins, N. E., Ziveri, P., Gray, W., Rae, J. W. B., Liu, X.,
1041   Byrne, R. H., Chen, S., Moore, C., Martell-Bonet, L., Steiner, Z., Antler, G., Hu, H., Lunstrum,

1042 A., Hou, Y., Kemnitz, N., Stutsman, J., Pallacks, S., Dugenne, M., Quay, P. D., Berelson, W. M.,
1043 and Adkins, J. F.: Shallow Calcium Carbonate Cycling in the North Pacific Ocean, Global
1044 Biogeochem Cycles, 36, 1–22, https://doi.org/10.1029/2022GB007388, 2022.
1045 Sulpis, O., Jeansson, E., Dinauer, A., Lauvset, S. K., and Middelburg, J. J.: Calcium carbonate
1046 dissolution patterns in the ocean, Nat Geosci, 14, 423–428, https://doi.org/10.1038/s41561-
1047 021-00743-y, 2021.
1048 Sulpis, O., Agrawal, P., Wolthers, M., Munhoven, G., Walker, M., and Middelburg, J. J.:
1049 Aragonite dissolution protects calcite at the seafloor, Nat Commun, 13, 1–8,
1050 https://doi.org/10.1038/s41467-022-28711-z, 2022.
1051 Torres, M. E., Hong, W. L., Solomon, E. A., Milliken, K., Kim, J. H., Sample, J. C., Teichert, B.
1052 M. A., and Wallmann, K.: Silicate weathering in anoxic marine sediment as a requirement for
1053 authigenic carbonate burial, Earth Sci Rev, 200, 102960,
1054 https://doi.org/10.1016/j.earscirev.2019.102960, 2020.
1055 Tyka, M. D., Van Arsdale, C., and Platt, J. C.: CO2 capture by pumping surface acidity to the
1056 deep ocean, Energy Environ Sci, 15, 786–798, https://doi.org/10.1039/d1ee01532j, 2022.
1057 Wallmann, K., Diesing, M., Scholz, F., Rehder, G., Dale, A. W., Fuhr, M., and Suess, E.: Erosion
1058 of carbonate-bearing sedimentary rocks may close the alkalinity budget of the Baltic Sea
1059 and support atmospheric CO2 uptake in coastal seas, Front Mar Sci, 9, 1–15,
1060 https://doi.org/10.3389/fmars.2022.968069, 2022.
1061 Zhong, S. and Mucci, A.: Calcite and aragonite precipitation from seawater solutions of
1062 various salinities: Precipitation rates and overgrowth compositions, Chem Geol, 78, 283–
1063 299, https://doi.org/10.1016/0009-2541(89)90064-8, 1989.
1064